Atmos. Meas. Tech. Discuss., 7, 1001–1025, 2014
www.atmos-meas-tech-discuss.net/7/1001/2014/
doi:10.5194/amtd-7-1001-2014

Atmospheric Measurement Techniques
Open Access
Discussions

Validation of the Aura High Resolution Dynamics Limb Sounder geopotential heights

L. L. Smith[1] and J. C. Gille[1,2]

[1]Atmospheric Chemistry Division, National Center for Atmospheric Research, Boulder, Colorado, USA
[2]Center for Limb Atmospheric Sounding, University of Colorado, Boulder, Colorado, USA

Received: 16 January 2014 – Accepted: 26 January 2014 – Published: 5 February 2014

Correspondence to: L. L. Smith (lsmith@ucar.edu)

Published by Copernicus Publications on behalf of the European Geosciences Union.

Abstract

Global satellite observations from the EOS Aura spacecraft's High Resolution Dynamics Limb Sounder (HIRDLS) of temperature and geopotential height (GPH) are discussed. The accuracy, resolution and precision of the HIRDLS version 7 algorithms are assessed and data screening recommendations are made. Comparisons with GPH from observations, reanalyses and models including European Center for Medium-Range Weather Forecasts Interim Reanalysis (ERA-Interim), National Centers for Environmental Prediction/National Center for Atmospheric Research (NCEP/NCAR) Reanalysis, Goddard Earth Observing System Model (GEOS) version 5, and EOS Aura Microwave Limb Sounder (MLS) illustrate the HIRDLS GPH have a precision ranging from 2 m to 30 m and an accuracy of ±100 m. Comparisons indicate HIRDLS GPH may have a slight low bias in the tropics and a slight high bias at high latitudes. Geostrophic winds computed with HIRDLS GPH qualitatively agree with winds from other data sources including ERA-Interim, NCEP and GEOS-5.

1 Introduction

The High Resolution Dynamics Limb Sounder (HIRDLS) instrument is an infrared limb-scanning radiometer onboard NASA's Aura satellite, launched on 15 July 2004. HIRDLS was designed to obtain high vertical and horizontal resolution observations in the upper troposphere, the stratosphere, and the lower mesosphere, at altitudes of 8–80 km. HIRDLS was proposed to address scientific issues of smaller-scale dynamical and chemical phenomena, particularly near the tropopause.

The HIRDLS instrument measures 6.12 to 17.76 micro-meter atmospheric limb emissions via 21 spectral channels to obtain vertical profiles of pressures, temperatures, and mixing ratios of 10 species as well as other quantities such as cloud top pressures and aerosol extinction at 12.1 micrometers. From the temperature profiles, geopotential height (GPH) profiles are computed.

Discussion Paper | Discussion Paper | Discussion Paper | Discussion Paper |

AMTD

7, 1001–1025, 2014

Validation of the Aura HIRDLS geopotential heights

L. L. Smith and J. C. Gille

To create HIRDLS Level 3 data we utilize an updated version of the Remsberg et al. (1990) Kalman filter algorithm on the HIRDLS level 2 profile data to create zonal Fourier coefficients, (see also Morris et al. (1995) and references therein). The resulting zonal Fourier coefficients are used to create mapped HIRDLS temperature and GPH on a $1^\circ \times 1^\circ$ latitude longitude grid. From the mapped GPH, the mapped geostrophic zonal and meridional winds are computed.

This paper is organized as follows. In Sect. 2, the HIRDLS temperature and Tangent Height at Nominal Altitude (THNA) measurements are described and the GPH calculation is outlined. This section also includes some data usage guidelines and a discussion of GPH precision. In Sect. 3, we briefly discuss comparisons of HIRDLS temperatures to other data sources and we compare HIRDLS GPH to other data sources including ERA-Interim, National Centers for Environmental Prediction/National Center for Atmospheric Research (NCEP/NCAR) Reanalysis, Goddard Earth Observing System Model (GEOS) version 5 and MLS. In Sect. 4, we compare geostrophic winds computed with HIRDLS GPH to other geostrophic winds including ERA-Interim and GEOS-5. Finally, in Sect. 5, we draw some conclusions.

2 HIRDLS temperature measurement and GPH calculation descriptions

2.1 The HIRDLS measurement system

HIRDLS utilizes the infrared limb scanning method, in which the radiance emitted by the atmosphere observed at the limb or horizon is measured as a function of relative altitude. Then, an algorithm processes the radiances to retrieve temperatures and trace constituents as a function of pressure, incorporating the hydrostatic relationship, over the range of altitudes for which the signal hasn't saturated and for which there is a good signal-to-noise ratio.

HIRDLS has 4 channels relevant to temperature which enables channels to be devoted to gases whose signals in the center of their bands saturate at low altitudes.

AMTD
7, 1001–1025, 2014

These channels in the more transparent band wings allow sounding of lower altitudes, including the desirable upper troposphere/lower stratosphere (UT/LS) region. Additionally, channels with minimal absorption by atmospheric gases can be utilized to observe particulates such as aerosols and clouds. Most importantly for the purposes of this study, more channels can be devoted to temperature sounding, which yields better results and provides redundancy.

Unfortunately, during launch, a piece of plastic Kapton film came loose and obscured the instrument aperture. The most definitive consequence of the blockage is that useful scans can only be obtained at the largest azimuth angle away from the Sun, or a line of sight (LOS) of 47° on the anti-Sun side of the orbital plane, looking backward. This limits the longitudinal resolution to the orbital spacing of 24.72°, prevents coverage south of 63° S and north of 80° N, and precludes simultaneous measurements with other A-Train instruments. However, the HIRDLS team has managed to obtain significant useful data, as outlined in Gille et al. (2008), and elsewhere, and as we will show here.

For Version 7, HIRDLS has released Level 3 data zonal Fourier coefficient data files, created by applying a Kalman filter mapping algorithm similar to that described by Rodgers (2000), Kohri (1981), and Remsberg et al. (1990). In this process each data point is used to update estimates of the zonal mean and coefficients of the sine and cosine coefficients of the first 7 zonal waves (15 values, equivalent to the mean plus amplitudes and phases of the first 7 zonal waves). This is done for each pressure level and zonal band going both forward and backward in time, and the results are combined, thus ensuring smooth time evolution. Values are output at one time of day, 12:00 UT, resulting in daily values of the estimated quantities every 1° in latitude. This produces an optimal estimate of the state of the system in this representation. In general the final estimated field will not go through the input points, but will have an RMS difference from them, termed the precision, approximately equal to the precision of the single profile observations. The output data includes this RMS value, as well as the values from each of the diagonal elements of the covariance matrix that give the predicted variance of each of the estimated quantities. The output data also includes the number of points that went into producing the estimate for that day. Since the Kalman estimator produces estimates even in the absence of data, a negative number of points indicates the number of days without data since (or until) a day with data, but the largest gap in this analysis is less than a day.

All HIRDLS data discussed here are from Version 7, available at the NASA GSFC Earth Sciences (GES) Data and Information Services Center (DISC): http://disc.sci.gsfc.nasa.gov/Aura/data-holdings/HIRDLS. Data discussed here are presented from 29 January 2005 until 17 March 2008, although occasional periods of less than a day are missing when various non-science scans were run for test purposes.

2.2 HIRDLS temperature measurements

The HIRDLS retrieval algorithm has been previously described by Khosravi et al. (2009) and references therein. Briefly, the retrieval algorithm is a maximum a posteriori retrieval (Rodgers, 2000) of the radiances determined from channels 2–5 (14.7–16.7 µm), following the physics described by Gille and House (1971). Input data is on a uniform altitude scale, while the solution returns the temperature and pressure at these levels, with the altitude and pressure hydrostatically consistent.

The retrieval starts from an initial guess and due to the Kapton film blockage, HIRDLS uses GEOS-5 assimilated meteorological data to provide LOS gradients as well as the first guess. On each iteration, the LOS gradient is fixed and the temperature at the tangent point is adjusted. For the a priori temperature the HIRDLS version 7 uses the GEOS v5.1.0 with an uncertainty of ±2 K down to and including the HIRDLS measured cloud top and ±20 K below that.

When the retrieval is completed, the data are interpolated to pressure levels, with 24 levels per pressure decade, uniformly spaced in log pressure.

AMTD
7, 1001–1025, 2014

2.3 HIRDLS GPH calculations

We calculate HIRDLS geopotential height via the standard $Z_j - Z_i = (R_d/g_0)_{pj} \int^{pi} T \, \mathrm{d}p/p$ where $Z_j - Z_i$ indicates GPH thickness between HIRDLS pressure layers and using as input the HIRDLS Level-2 Temperatures and HIRDLS Tangent Height at Nominal Altitude. The Tangent Height at Nominal Altitude (THNA) is obtained by calling the Science Data Processing (SDP) Toolkit software from NASA for each radiance and choosing the resulting sample closest to 30 km (Noerdlinger, 1995). Notice that the HIRDLS GPHs are calculated utilizing only Aura satellite data. This paper is thus a test of this method.

The resulting HIRDLS Geopotential Heights have high vertical resolution, based on the high vertical resolution of HIRDLS temperature/pressure profiles. An averaging-kernel characterization of the retrieved temperatures gives a vertical resolution of 1–1.2 km and the pressure profiles (with vertical resolution ∼ 0.7 km) are retrieved using the corresponding retrieved temperature profiles, so they have approximately the same resolution. The predicted GPH precision is computed similarly utilizing the predicted temperature precisions. As with the temperatures, in the stratosphere, the geopotential height precision is independent of latitude and season, and varies from only slightly in the upper troposphere to about the stratopause, above which it grows slightly, depending on latitude and season.

Figure 1 illustrates the predicted GPH precision estimated as follows: the chain rule applied to the standard GPH algorithm yields the predicted GPH precision per pressure level in terms of quantities such as the temperature precisions. Then the precision of GPH on each pressure level is computed by taking the square-root of the sum of the squares that contribute to that level. In this figure data used were from the equinoxes and solstices for years 2005–2007. The minimum in the predicted GPH precision at approximately 10 hPa corresponds to the location of the THNA. Notice the predicted precision increases as we move away from the THNA because each successive layer adds a contribution.

AMTD
7, 1001–1025, 2014

Since the HIRDLS Version 7 GPH are computed with respect to the ellipsoid, for the purposes of this paper we modify them by utilizing the Earth Gravitational Model and subtracting the geoid heights above the ellipsoid (National Geospatial Intelligence Agency, 2008) to get the GPH with respect to the geoid.

3 Validation of geopotential heights

An earlier version of HIRDLS Temperatures, Version 3, was validated by Gille et al. (2008) via comparisons with data from high-resolution sondes, lidars, the Atmospheric Chemistry Experiment Fourier Transform Spectrometer (ACE-FTS) and reanalyses. They conclude the HIRDLS temperatures are within ±2 K of standard temperatures from the upper troposphere to the upper stratosphere, with the possible exception of the tropical tropopause region. HIRDLS temperatures show no indication of latitudinal variations of biases or temporal drifts. Moreover, the noise levels are consistent with predictions and low enough to make the data highly useful. Furthermore, the HIRDLS temperatures show an ability to resolve small vertical scales and capture atmospheric wave motions as discussed by Wright et al. (2011) for gravity waves and Alexander and Ortland (2010) for equatorial waves, for example.

As discussed in Gille et al. (2013), overall, the version 7 HIRDLS temperatures have a precision between ≤ 0.5 K (lower stratosphere) to > 3 K (mesopause) and are accurate to ≤ 1 K from the 300–400 hPa to 1 hPa, becoming cooler above that level.

In the original HIRDLS Measurements Requirements (Gille et al., 1997) it was proposed that the horizontal geopotential height gradient should be on the order of 20 m/500 km, or stated another way, the derivatives with respect to latitude of the differences of HIRDLS GPH with a standard dataset must be smaller than $\pm 0.04\,\mathrm{m\,km^{-1}}$. This requirement enables one to compute geostrophic wind, at 60° N, for example, to better than $3\,\mathrm{m\,s^{-1}}$. Figure 2a illustrates the mean latitudinal derivatives of HIRDLSv7 GPH differenced with ERA-Interim GPH, for two sample pressure levels, averaged over the entire mission. While there is significant latitudinal variation, the released GPH are

AMTD
7, 1001–1025, 2014

thus consistent with the original measurement requirements. Figure 2b illustrates the mean longitudinal derivatives of HIRDLSv7 GPH differenced with ERA-Interim GPH, for two sample pressure levels, averaged over the entire mission. There is little variation in the longitudinal case.

Since HIRDLS GPH are calculated via the HIRDLS temperatures, their scientifically useful pressure range is the same as the HIRDLS temperatures: 1000 hPa to 0.01 hPa. HIRDLS GPH have been compared to several data sets in an effort to determine the extent and magnitude of any bias. For example, we compare HIRDLSv7 zonal mean GPH with the GPH of other standard datasets. In Fig. 3a, we see the differences of HIRDLSv7 zonal mean GPH with ERA-Interim zonal mean for all ERA-Interim-available vertical levels for 2005 through 2007. Notice the HIRDLSv7 GPH are scientifically useful up to and including 0.01 hPa, but comparison data sets at these levels are difficult to obtain. In general the ERA-Interim comparison indicates HIRDLSv7 GPH is lower in the tropics and higher at higher latitudes. In Fig. 3b we see the standard deviation of the differences with ERA-Interim for 2005 through 2007. The standard deviation does not vary much with latitude. The maxima in the standard deviations at $\sim$ 10 mb are due to the HIRDLS THNA at that pressure level, which we integrate from. The ERA-Interim GPH does not have a similar reference level. Thus the standard deviations decrease as we move away from 10 mb.

In Fig. 4a, we see the mean differences for 2005 through 2007, of HIRDLSv7 zonal mean GPH with NCEP zonal mean GPH. In general the pattern indicates HIRDLSv7 GPH is lower in the tropics and higher at higher latitudes. In Fig. 4b we see the standard deviation of the differences with NCEP/NCAR Reanalysis for 2005 through 2007. The NCEP differences and standard deviations are smoother than those with respect to ERA-Interim because the NCEP data has a coarser vertical resolution; thus, when interpolating to the NCEP levels to enable comparisons, the differences are essentially smoothed and the artifact from the THNA isn't noticeable.

The mean differences of zonal mean HIRDLSv7 GPH with respect to GEOS5 and Whole Atmosphere Community Climate Model (WACCM) (not shown) are similar to

AMTD
7, 1001–1025, 2014

the ERA-Interim comparisons. Overall, from the zonal mean comparisons, the HIRDLS version 7 GPH appears to have a slight positive bias at high latitudes and a slight low bias in the tropics. It's not immediately apparent why this might be since the HIRDLS version 7 temperatures did not show a similar bias.

The HIRDLS team also creates $1^{\circ} \times 1^{\circ}$ latitude longitude maps with its Level 3 Zonal Fourier Coefficients data utilizing the Kalman filter mapping algorithm as discussed above. Thus, we synthesize the latitude longitude maps for GPH and compare to other standard global GPH data. Figure 5a shows the Version 7 HIRDLS GPH Mercator map for sample day 18 May 2006, for two sample pressure levels, 1 mb and 100 mb. These levels are chosen because standard global GPH datasets also include these levels and thus no vertical interpolation is required for comparisons.

Figure 5b and c illustrate the ERA-Interim GPH Mercator map for sample day 18 May 2006, for the same two pressure levels, 1 mb and 100 mb. The latitudinal and longitudinal variations of the ERA-Interim data are very similar to those of the HIRDLSv7 data. Both sets of data show the expected Southern Hemisphere high latitude minima for this day at 1 mb and 100 mb as well as the maxima at the tropics at 100 mb. This figure (bottom row) also illustrates the difference of HIRDLSv7 GPH and ERA-Interim GPH. Note the maximum values in the difference plots are on the order of ±100 m or less.

Mercator map GPH plots and differences with HIRDLSv7, for similar levels and this sample day, 2006d138, with GEOS5, WACCM and NCEP/NCAR Reanalysis data (not shown) are very similar. Overall, the Mercator map plots at 100 mb may support a slight negative bias in HIRDLS version 7 GPH in the tropics, with a slight positive bias at high latitudes, consistent with the zonal mean comparisons. Overall, the Mercator map plots at 1 mb seem to indicate only a slight positive bias at high southern latitudes.

For a sample day in the winter season, we consider 21 December 2006. Thus Fig. 6 illustrates the HIRDLSv7 (top row), ERA-Interim (middle row) GPH polar stereographic map for sample day 2006d355, for the same two pressure levels, 1 mb and 100 mb. The latitudinal and longitudinal variations of the ERA-Interim data are very similar to those

AMTD
7, 1001–1025, 2014

of the HIRDLSv7 data. Both sets of data show the expected Northern Hemisphere minima for this day at 1 mb and 100 mb. This figure also illustrates the difference of HIRDLSv7 GPHs and ERA-Interim GPHs (bottom row). Note the maximum values in the difference plots are less than or on the order of ±100 m and the HIRDLS data seem to show more fine structure. It is not know if this fine structure is physical. Notice that the gradients in the difference plots are relatively small.

Polar stereographic map GPH plots, and differences with HIRDLSv7, for similar levels and this sample day, 2006d355, with GEOS5, WACCM and NCEP/NCAR Reanalysis data (not shown) are similar. Generally, the polar stereographic plots at these levels show HIRDLS version 7 GPH have a minor low bias in the Northern Hemisphere, i.e. HIRDLS is cooler, with the exception of the highest latitudes.

To check for any possible overall biases we computed mean GPH differences with ERA-Interim GPH for 2005 through 2007, shown in Fig. 7. There appear to be biases near the equator, where mapped HIRDLSv7 GPH are too low for all vertical levels. At high latitudes, HIRDLSv7 GPH appear too high for all vertical levels. HIRDLSv7 GPH differences with NCEP/NCAR Reanalyses GPH for 2005 through 2007 (not shown) show the same biases. Notice, however, all these biases are quantitatively on the order of 1 % or less of the geopotential height values. Again, the gradients of the differences appear to be small.

On the whole, the HIRDLS version 7 GPH agree quite well with other datasets. This would appear to validate the HIRDLS method of computing GPH from temperatures and THNA. The HIRDLS version 7 GPH appear to have a slight low bias in the tropics and a slight high bias at high latitudes. Since the HIRDLS version 7 temperatures did not show this bias, possibly it comes from the THNA. This deserves further study.

4 Comparison of geostrophic winds with other data sources

As an additional test of the HIRDLS version 7 geopotential heights, one can compute the geostrophic winds from HIRDLSv7 GPH and compare the results to standard

AMTD
7, 1001–1025, 2014

datasets. Of course, the Coriolis factor means this method will not produce usable winds in the tropics.

In Fig. 8a, we see the zonal winds derived from HIRDLSv7 for sample day 18 May 2006 and sample pressure levels 1 mb and 100 mb (top row), in Fig. 8b, we see ERA-Interim for the same sample day and levels (middle row), and Fig. 8c shows their differences (bottom row). In Fig. 8a and b, notice the large maxima at high southern latitudes and the band of minima along 30° N for the 1 mb case. For the 100 mb case, we see maxima at high latitudes, with some spots of minima in the tropics. Qualitatively, these plots agree very well. Regarding Fig. 8c, the differences show no systematic biases, and most differences are less than or on the order of $\pm 5\,\mathrm{m\,s^{-1}}$.

Mercator map GPH plots for this sample day and similar levels for NCEP, GEOS5 and WACCM zonal winds and their differences with HIRDLSv7-derived zonal geostrophic winds (not shown) are very similar. Overall, the differences of HIRDLS version 7 zonal wind with other zonal winds for this sample day and these levels show no systematic biases, and most differences are less than or on the order of $\pm 5\,\mathrm{m\,s^{-1}}$, consistent with the ERA-Interim case, above.

To double-check any possible temporal biases we computed these zonal wind differences for 2005 through 2007, as shown in Fig. 9. The only significant biases are found near the equator where the Coriolis factor introduces nonphysical results.

In Fig. 10a we see the geostrophic meridional winds computed from HIRDLSv7 GPHs for sample day 18 May 2006 and sample pressure levels 1 mb and 100 mb (top row), Fig. 10b shows the meridional winds from ERA-Interim for sample day 18 May 2006 and sample pressure levels 1 mb and 100 mb (middle row), with their differences in Fig. 10c (bottom row). The large maxima and minima coincide for the most part with the HIRDLSv7-derived meridional winds. Thus the large-scale pattern agrees.

Mercator map GPH plots for this sample day and similar levels for NCEP, GEOS5 and WACCM meridional winds and their differences with HIRDLSv7-derived meridional geostrophic winds (not shown) are similar.

AMTD
7, 1001–1025, 2014

L. L. Smith and J. C. Gille

We examine the mean meridional wind differences for 2005 through 2007, and their standard deviations at 1 mb and 100 mb, as shown in Fig. 11a and b. Again, there are significant biases found near the equator where the Coriolis factor introduces nonphysical results. For the meridional winds, however, these biases appear to propagate to slightly higher latitudes, as shown in the difference plots.

Since, however, the HIRDLS version 7 GPH–derived geostrophic winds, particularly zonal winds, agree well with other winds away from the tropics, this would also seem to indicate the HIRDLS version 7 GPH are scientifically useful.

5 Conclusions

The version 7 HIRDLS geopotential heights are considered scientifically useful at pressures from 1000 hPa to 0.01 hPa. Data comparisons indicate the HIRDLS GPH have a altitude-dependent precision ranging from 2 m to 30 m and an accuracy of ±100 m, and the HIRDLS GPH may have a slight low bias in the tropics and a slight high bias at high latitudes, of less than 1 %. Therefore, HIRDLS version 7 GPH have good precision and accuracy. This satellite data set should be quite useful for scientific studies.

Acknowledgements. The authors would like to thank the entire HIRDLS team for excellent work in a challenging situation. We'd also like to thank L. Henderson for help with this paper.

The graphics here were made with The NCAR Command Language (Version 6.1.2) (Software) (2013). Boulder, Colorado: UCAR/NCAR/CISL/VETS. doi:10.5065/D6WD3XH5.

The European Centre for Medium-range Weather Forecasting (ECMWF) ERA-Interim assimilated data for this study is from the Research Data Archive (RDA) which is maintained by the Computational and Information Systems Laboratory (CISL) at the National Center for Atmospheric Research (NCAR). NCAR is sponsored by the National Science Foundation (NSF). The original data are available from the RDA (http://dss.ucar.edu) in dataset number ds627.0.)

The National Center for Atmospheric Research is sponsored by the National Science Foundation. Any opinions, findings and conclusions or recommendations expressed in the publication are those of the author(s) and do not necessarily reflect the views of the National Science Foundation.

References

Alexander, M. J. and Ortland, D. A.: Equatorial waves in High Resolution Dynamics Limb Sounder (HIRDLS) data, J. Geophys. Res. Atmos., 115, D24111, doi:10.1029/2010JD014782, 2010.

Gille, J. C. and House, F. B.: On the inversion of limb radiance measurements, I. Temperature and thickness, J. Atmos. Sci., 28,1427–1442, 1971.

Gille, J. C., Barnett, J. J., and Boville, B.: The Science Requirements Document, SC-HIR-012C, Oxford University and University of Colorado, Boulder, available at: http://www.eos.ucar.edu/hirdls (last access: 3 February 2014), 1997.

Gille, J. C., Barnett, J., Arter, P., Barker, M., Bernath, P., Boone, C., Cavanaugh, C., Chow, J., Coffey, M., Craft, J., Craig, C., Dials, M., Dean, V., Eden, T., Edwards, D. P., Francis, G., Halvorson, C., Harvey, L., Hepplewhite, C., Khosravi, R., Kinnison, D., Krinsky, C., Lambert, A., Lee, H., Lyjak, L., Loh, J., Mankin, W., Massie, S., McInerney, J., Moorhouse, J., Nardi, B., Packman, D., Randall, C., Reburn, J., Rudolf, W., Schwartz, M., Serafin, J., Stone, K., Torpy, B., Walker, K., Waterfall, A., Watkins, R., Whitney, J., Woodard, D., and Young, G.: High Resolution Dynamics Limb Sounder: experiment overview, recovery, and validation of initial temperature data, J. Geophys. Res., 113, D16S43, doi:10.1029/2007JD008824, 2008.

Gille, J. C., Gray, L., Cavanaugh, C., Coffey, M., Dean, V., Halvorson, C., Karol, S., Khosravi, R., Kinnison, D., Massie, S., Nardi, B., Belmonte Rivas, M., Smith, L., Torpy, B., Waterfall, A., and Wright, C.: High Resolution Dynamics Limb Sounder Earth Observing System (EOS) Data Description and Quality Version 7, available at: http://disc.sci.gsfc.nasa.gov/Aura/data-holdings/HIRDLS/documents/HIRDLS-V7-DQD.pdf (last access: 3 February 2014) 2013.

Khosravi, R., Lambert, A., Lee, H., Gille, J., Barnett, J., Francis, G., Edwards, D., Halvorson, C., Massie, S., Craig, C., Krinsky, C., McInerney, J., Stone, K., Eden, T., Nardi, B., Hepplewhite, C., Mankin, W., and Coffey, M.: Overview and characterization of retrievals of Temperature and atmospheric constituents from HIRDLS measurements, J. Geophys. Res., 114, D20304, doi:10.1029/2009JD011937, 2009.

Kohri, W. J.: LRIR Observations of the Structure and Propagation of the Stationary Planetary Waves in the Northern Hemisphere during December 1975, Cooperative Thesis No. 63, Drexel University and National Center for Atmospheric Research, 1981.

Morris, G. A., Schoeberl, M. R., Sparling, L. C., Newman, P. A., Lait, L. R., Elson, L., Waters, J., Suttie, R. A., Roche, A., Kumer, J., and Russell, J. M.: Trajectory mapping and applications to data from the upper-atmosphere research satellite, J. Geophys. Res., 100, D16491, doi:10.1029/95JD01072, 1995.

Noerdlinger, P. D.: Theoretical Basis of the SDP Toolkit Geolocation Package for the ECS Project, 445-TP-002-002, see also: NASA SDP Toolkit/HDF-EOS EOSDIS Core System Project, available at: http://newsroom.gsfc.nasa.gov/sdptoolkit/toolkit.html (last access: 3 February 2014), 1995.

The National Geospatial Intelligence Agency: Earth Gravitational Model, available at: http://earth-info.nga.mil/GandG/wgs84/gravitymod/egm2008/egm08_wgs84.html (last access: 3 February 2014), 2008.

Remsberg, E. E., Haggard, K. V., and Russell III, J. M.: Estimation of synoptic fields of middle atmosphere parameters from Nimbus-7 LIMS Profiles Data, J. Atmos. Ocean. Tech., 7, 689–705, doi:10.1175/1520-0426(1990)007<0689:EOSFOM>2.0.CO;2 1990.

Rodgers, C. D.: Inverse Methods for Atmospheric Sounding, Theory and Practice, World Sci., Hackensack, NJ, 2000.

Wright, C. J., Rivas, M. B., and Gille, J. C.: Intercomparisons of HIRDLS, COSMIC and SABER for the detection of stratospheric gravity waves, Atmos. Meas. Tech., 4, 1581–1591, doi:10.5194/amt-4-1581-2011, 2011.

AMTD

7, 1001–1025, 2014

Validation of the Aura HIRDLS geopotential heights

L. L. Smith and J. C. Gille

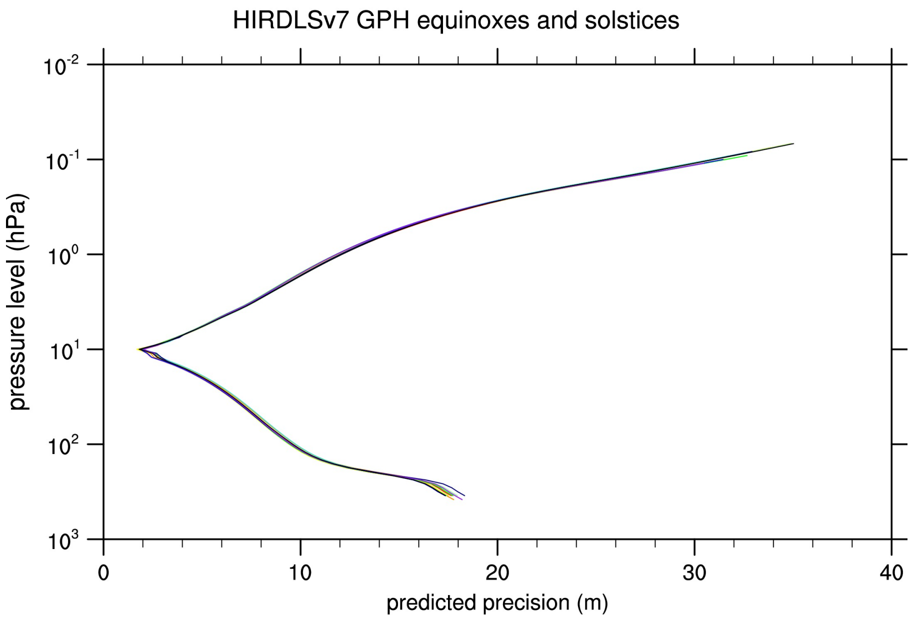

Fig. 1. Predicted precision (m) of HIRDLS V7 GPH for 12 equinoxes and solstices 2005–2007.

AMTD
7, 1001–1025, 2014

Validation of the Aura HIRDLS geopotential heights

L. L. Smith and J. C. Gille

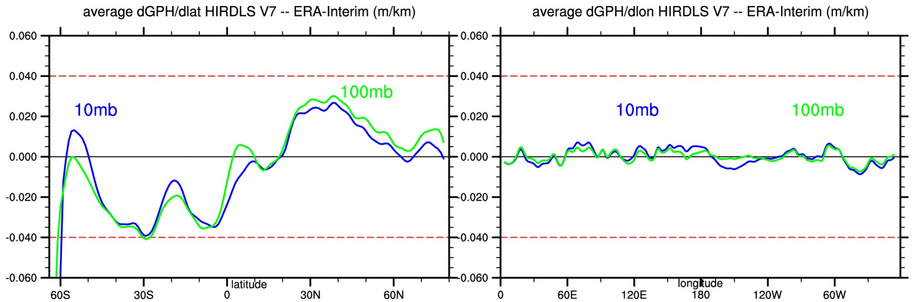

Fig. 2. Derivatives of the differences of HIRDLSv7 GPH with ERA-Interim at 10 mb and 100 mb for the entire HIRDLS mission, with respect to **(a)** latitude and **(b)** longitude.

AMTD
7, 1001–1025, 2014

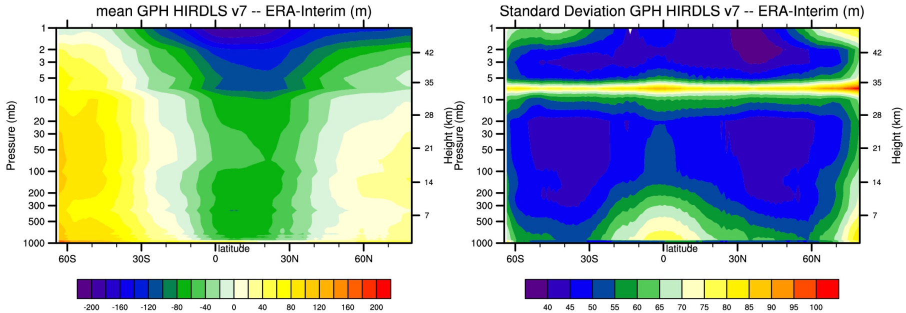

Fig. 3. **(a)** Mean differences of zonal mean HIRDLSv7 GPH with respect to ERA-Interim for 2005–2007, **(b)** standard deviations of same differences, all in meters.

AMTD
7, 1001–1025, 2014

Validation of the Aura HIRDLS geopotential heights

L. L. Smith and J. C. Gille

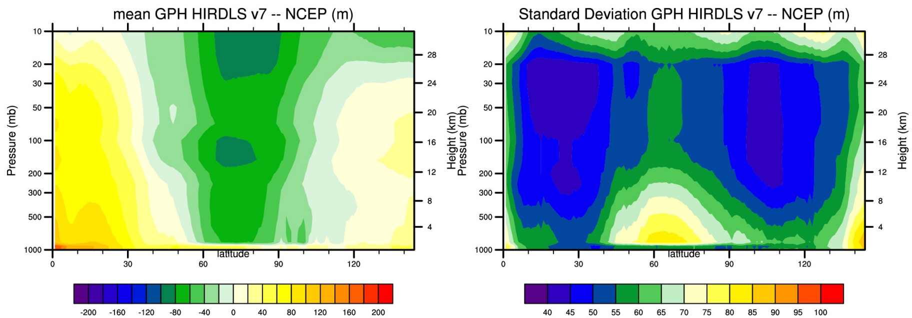

Fig. 4. (a) Mean differences of zonal mean HIRDLSv7 GPH with respect to NCEP for 2005–2007, **(b)** standard deviations of same differences, all in meters.

AMTD
7, 1001–1025, 2014

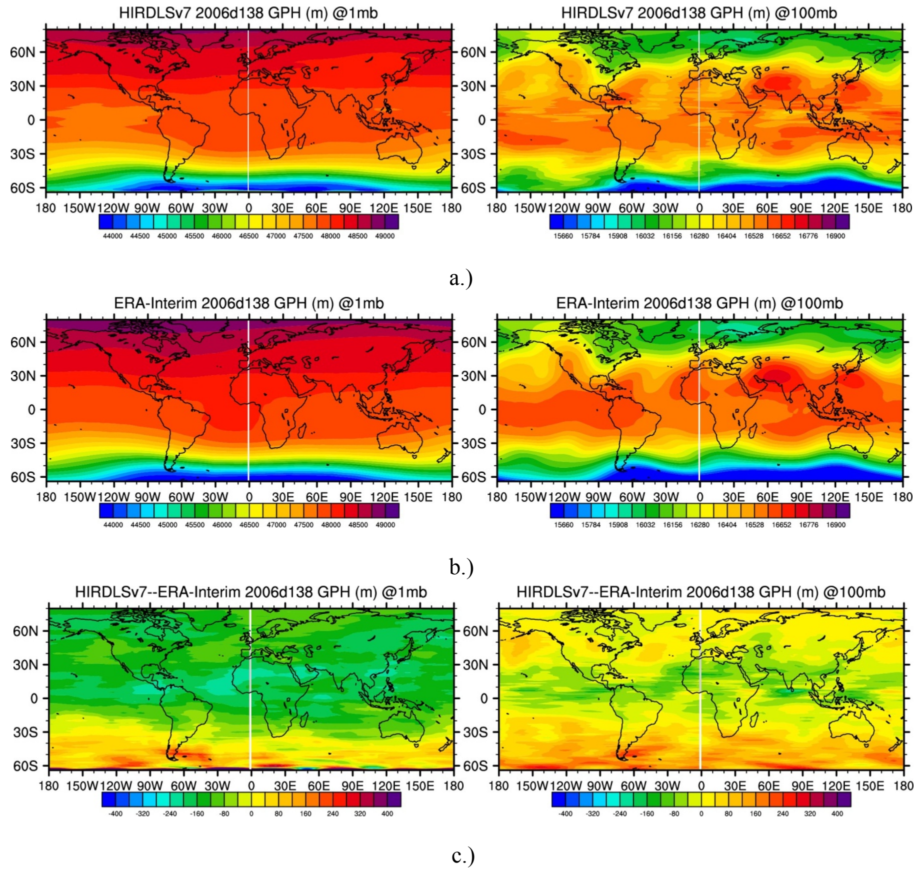

Fig. 5. (a) HIRDLS mapped GPHs for sample day 2006d138 at 1 mb and 100 mb, **(b)** ERA-Interim mapped GPHs for the same sample day and levels, and **(c)** differences, all in meters.

AMTD
7, 1001–1025, 2014

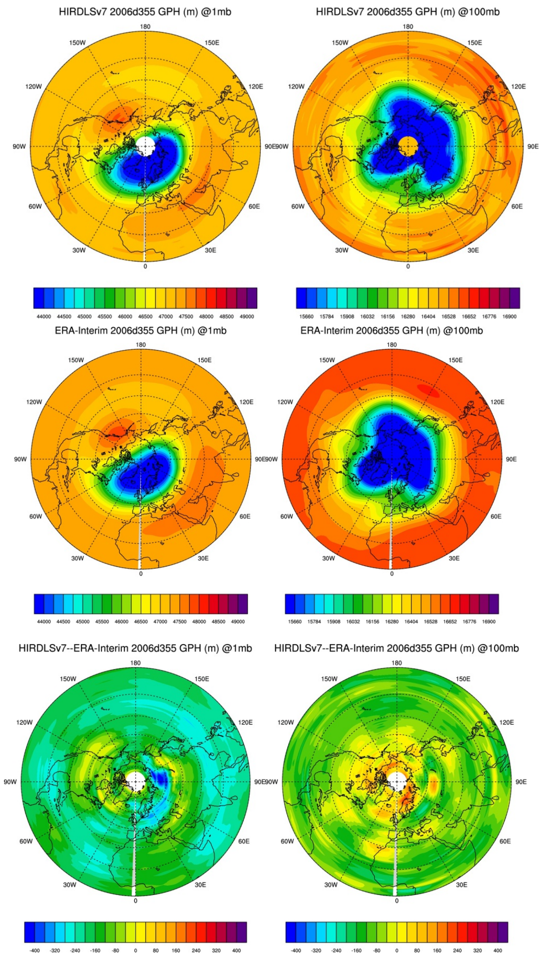

Fig. 6. HIRDLSv7 (top row), ERA-Interim (middle row) mapped GPHs for sample day 2006d355 at levels 1 mb and 100 mb, and differences (bottom row), all in meters.

AMTD
7, 1001–1025, 2014

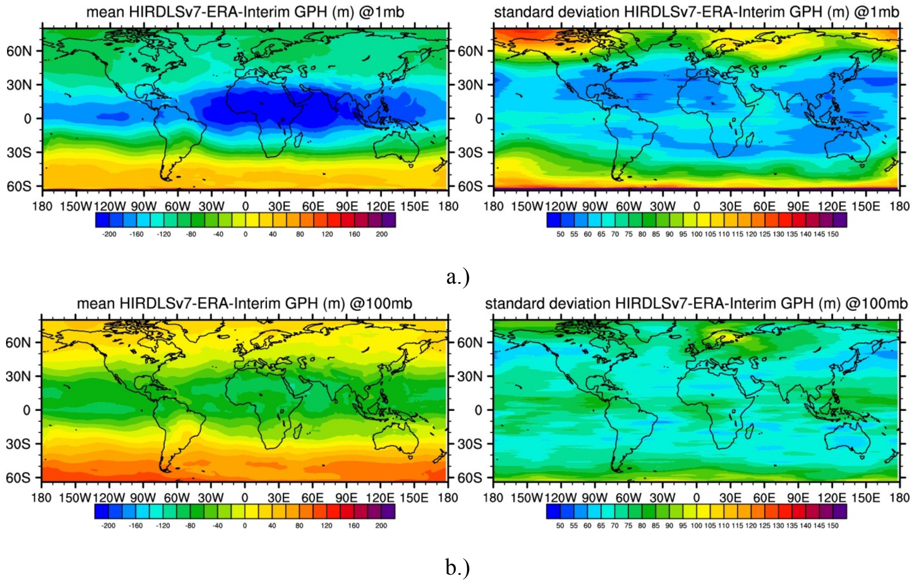

Fig. 7. Mean HIRDLSv7 GPHs minus ERA-Interim GPHs and their standard deviation for 2005 through 2007, at **(a)** 1 mb (top row), and **(b)** 100 mb (bottom row), all in meters.

AMTD
7, 1001–1025, 2014

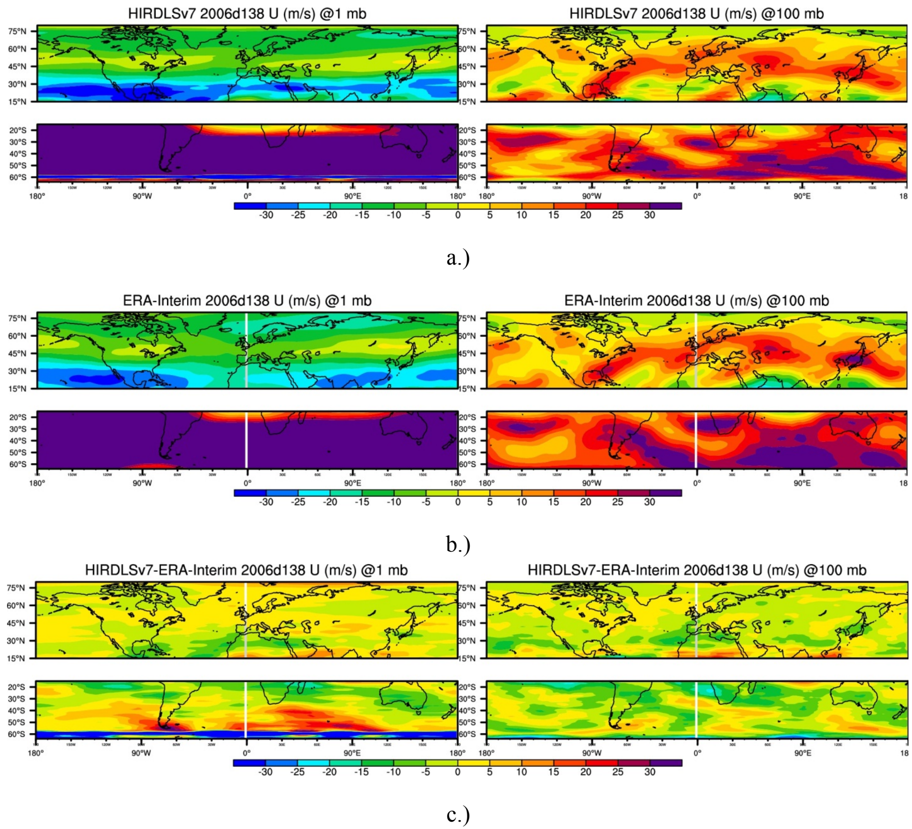

Fig. 8. (a) HIRDLSv7 mapped zonal geostrophic winds for sample day 2006d138 at levels 1 mb and 100 mb, **(b)** ERA-Interim mapped zonal winds for the same sample day and levels, **(c)** HIRDLSv7 – ERA-Interim mapped zonal winds for same sample day and levels, all in meters per second.

AMTD
7, 1001–1025, 2014

Validation of the Aura HIRDLS geopotential heights

L. L. Smith and J. C. Gille

AMTD
7, 1001–1025, 2014

Validation of the Aura HIRDLS geopotential heights

L. L. Smith and J. C. Gille

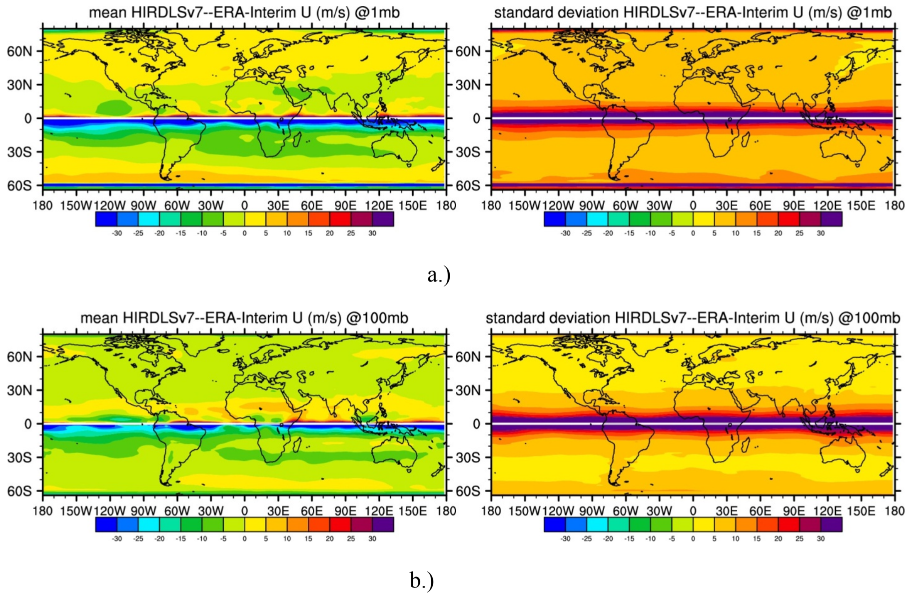

Fig. 9. Mean HIRDLSv7 geostrophic zonal winds minus ERA-Interim mapped zonal winds and their standard deviation for 2005 through 2007, at **(a)** 1 mb (top row) and **(b)** 100 mb (bottom row), all in meters per second.

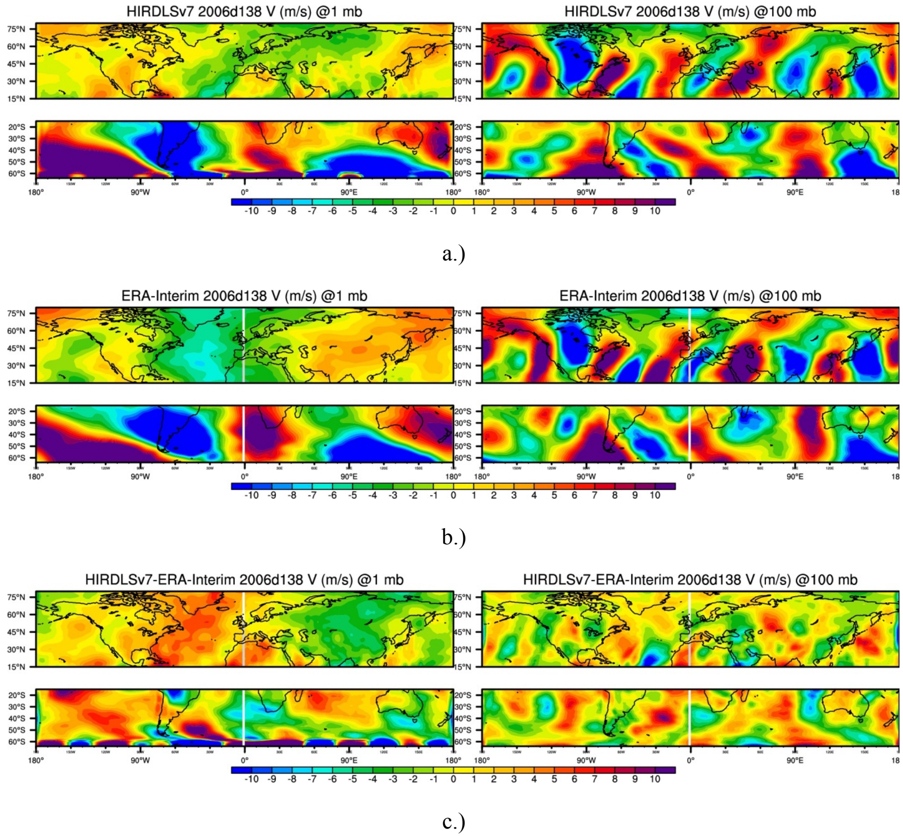

Fig. 10. (a) HIRDLS mapped meridional geostrophic winds for sample day 2006d138 at 1 mb and 100 mb, **(b)** ERA-Interim mapped meridional winds for the same sample day and levels, and **(c)** their differences, all in meters per second.

AMTD
7, 1001–1025, 2014

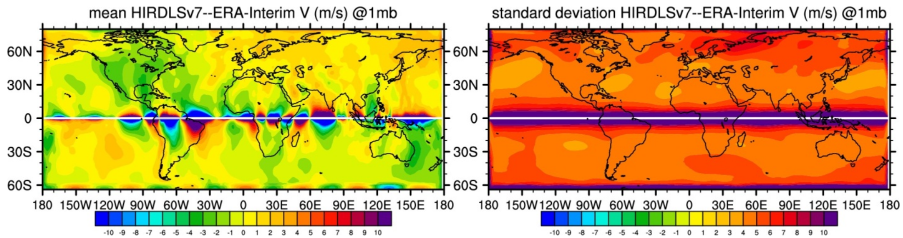

a.)

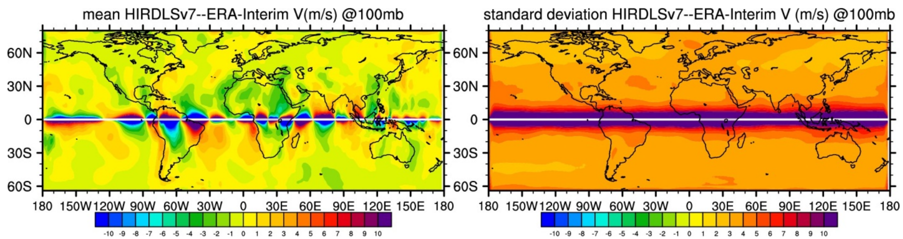

b.)

Fig. 11. Mean HIRDLSv7 geostrophic meridional winds minus ERA-Interim meridional winds and their standard deviations for 2005 through 2007, at **(a)** 1 mb (top row) and **(b)** 100 mb (bottom row), all in meters per second.

AMTD
7, 1001–1025, 2014